DYNAMICS OF SIS–EPIDEMIC MODEL WITH COMPETITION INVOLVING FRACTIONAL-ORDER DERIVATIVE WITH POWER-LAW KERNEL

ISMAIL DJAKARIA[1,*], HASAN S. PANIGORO[2], EBENEZER BONYAH[3], EMLI RAHMI[2], WAHAB MUSA[4]

[1]Magister Mathematics Education Programme, Post-Graduate, Universitas Negeri Gorontalo,

Gorontalo 96128, Indonesia

[2]Biomathematics Research Group, Department of Mathematics, Faculty of Mathematics and Natural Sciences,

Universitas Negeri Gorontalo, Bone Bolango 96119, Indonesia

[3]Department of Mathematics Education, Akenten Appiah-Menka University of Skills Training and

Entrepreneurial Development, Kumasi 00233, Ghana

[4]Department of Electrical Engineering, Universitas Negeri Gorontalo, Gorontalo 96128, Indonesia

Abstract. Infectious disease and competition play important roles in the dynamics of a population due to their capability to increase the mortality rate for each organism. In this paper, the dynamical behaviors of a single species population are studied by considering the existence of the infectious disease, intraspecific competition, and interspecific competition. The fractional-order derivative with a power-law kernel is utilized to involve the impact of the memory effect. The population is divided into two compartments namely the susceptible class and the infected class. The existence, uniqueness, non-negativity, and boundedness of the solution are investigated to confirm the biological validity. Three types of feasible equilibrium points are identified namely the origin, the disease-free, and the endemic points. All biological conditions which present the local and global stability are investigated. The global sensitivity analysis is given to investigate the most influential parameter to the basic reproduction number and the density of each class. Some numerical simulations including bifurcation diagrams and time series are also portrayed to explore more the dynamical behaviors.

*Corresponding author

E-mail address: iskar@ung.ac.id

1

1. INTRODUCTION

The spread of infectious disease still becomes a fundamental issue not only because of the existence of the population but also to maintain the balance of biological systems. Several scientific methods are developed to discover better ways to suppress and control the rate of disease infection [1]. The preferred ways for the last decades for this epidemiological problems are given by mathematical approach using a deterministic model which is considered efficacious to understand the mechanisms of disease transmission and evaluate the appropriate control strategies [2, 3, 4]. The fundamental one which has become the basis of epidemiological modeling is given by [5] which develops the continuous-time deterministic model using first-order derivative as the operator. This model is successfully developed in couple of ways such as the continuous-time single species epidemiological modeling with first-order derivative [6, 7, 8, 9], the discrete-time single species epidemiological modeling [10, 11, 12], the stochastic single-species epidemiological modeling [13, 14], and the continuous-time eco-epidemiological modeling [15, 16, 17].

Apart from those operators, several researchers prefer to use the fractional-order derivative to accomplish their problems the biological modeling. See [18, 19, 20] and references therein for some examples in epidemiological modeling. The fractional-order derivative is chosen by considering the capability of this operator to describe the current state of the biological object as the impact of all of its previous conditions which are known as the memory effect [21, 22]. In the epidemiological model, the transmission of disease may slow down and be forestalled by the susceptible population as the impact of the memory [23]. Some fractional-order derivative has been developed and successfully applied in epidemiological modeling such as the Riemann-Liouville, Caputo, Caputo-Fabrizio, and Atangana-Baleanu [24, 25, 26, 27]. From all of the given operators, the Caputo fractional-order derivative has the complete tools for dynamical analysis such as the existence and uniqueness, non-negativity and boundedness, local dynamics, global dynamics, and some bifurcation analysis. Consequently, the Caputo operator will be used in this paper where defined later in the next section.

In this work, we develop the epidemiological model based on the SIR model given by [5]. For single-species conditions, this model is only popular for the infectious diseases that appeared in the human population. In facts, infectious diseases also threaten the existence of the animal population which disturbs the balance of the ecosystem. For examples, the infectious diseases in endemic species such as Orangutans [28], Tarsius [29], Sumatran Tiger [30], and Komodo dragon [31]. Moreover, the natural behaviors of animals that endanger the existence of their populations are the intraspecific competition among them to preserve their food sources [32, 33, 34]. For these reasons, developing and investigating the dynamics of the epidemiological model by considering the impact of intraspecific competition and the memory effect are critical issues that become the novelty of our research.

The whole of this paper is organized in the following procedure: In Section 2, the mathematical modeling consists of model formulation, existence, uniqueness, non-negativity, and boundedness are given. The analytical results including the existence of equilibrium points and their local and global dynamics are completely investigated in Section 3. To show the most influential parameter of the model, the global sensitivity analysis is provided by Section 4. Some numerical simulations as well as bifurcation diagrams and time-series are presented in Section 5 to explore more about the dynamical behaviors of the model. This work ends by giving a conclusion in Section 6.

2. MATHEMATICAL MODELING

This section studies about mathematical modeling consisting of the model formulation, existence, uniqueness, non-negativity, and boundedness of solution. The mathematical model is constructed by a deterministic approach using a differential equation. We first give some assumptions to restrain the model so it does not get too complicated. We next interpret the giving assumptions to the mathematical formula using the first-order derivative as the operator. A diagram is presented to show the impact of each assumption on the flow of population density for each compartment. To involve the impact of the memory effect, the Caputo fractional-order derivative is applied to the model. For the mathematical model's validity, we show that the solution of the model always exists, unique, non-negative, and bounded.

2.1. Model Formulation. In this work, the model is constructed from a single population growth model. We first assume there exists a population in a habitat that grows proportionally to its density and bounded due to the intraspecific competition. Let $N(t)$ be the population at time t, r is the birth rate, μ is the natural death rate, and ω is the death rate as a result of competition. Thus, we have a first-order differential equation as follows.

$$\frac{dN}{dt} = (r - \mu)N - \omega N^2. \tag{1}$$

Next, we assume that the population is exposed by infectious disease. The population N is divided into two compartments namely the susceptible class (S) and infected class (I) where $N = S + I$. The susceptible class is infected by disease bilinearly with infection rate β. The competition is divided into two cases namely the intraspecific competition for each susceptible and infected class, and the interspecific competition between susceptible and infected classes. As result, the following model is received.

$$\begin{aligned} \frac{dS}{dt} &= (r - \mu)S - \omega_1 S^2 - (\omega_2 + \beta)SI, \\ \frac{dI}{dt} &= (\beta - \omega_4)SI - \omega_3 I^2 - \mu I, \end{aligned} \tag{2}$$

where ω_i, $i = 1, 2$ respectively denote the death rate of the susceptible population as the results of intraspecific and interspecific competitions between susceptible and susceptible classes, and susceptible and infected classes. The parameters ω_i, $i = 3, 4$ denote the death rate of the infected population as the result of competition between infected and infected classes, and susceptible and infected classes. In our works, we also assume that each organism has the capability to survive the disease. Thus, we define η as the recovery rate. Since each organism that survives from the disease has a chance to be re-infected, this type of population will be again susceptible. Finally, we have a mathematical model as follows.

$$\begin{aligned} \frac{dS}{dt} &= (r - \mu)S - \omega_1 S^2 - (\omega_2 + \beta)SI + \eta I, \\ \frac{dI}{dt} &= (\beta - \omega_4)SI - \omega_3 I^2 - (\eta + \mu)I. \end{aligned} \tag{3}$$

All of the given assumptions and their mathematical modeling are described in Figure 1.

Now, the Caputo fractional-order derivative will be applied in order to conduct the impact of the memory effect on the population growth rate. The similar procedure is adopted from
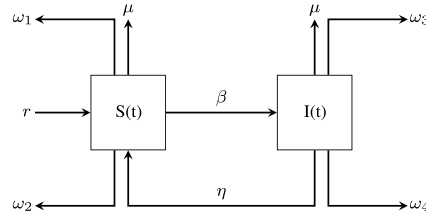
FIGURE 1. Compartment diagram of model (3)

[35]. The first-order derivatives on the left-hand side of model (3) are replaced by the Caputo fractional-order derivative defined as follows.

Definition 1. [36] Suppose $0 < \alpha \leq 1$. The Caputo fractional derivative of order$-\alpha$ is defined by

$$(4) \qquad {}^{C}\mathscr{D}_{t}^{\alpha} f(t) = \frac{1}{\Gamma(1-\alpha)} \int_{0}^{t} (t-s)^{-\alpha} f'(s)\,ds,$$

where $t \geq 0$, $f \in C^{n}([0,+\infty),\mathbb{R})$, and Γ is the Gamma function.

Applying Definition 1 to eq. (3), the following model is obtained.

$$(5) \qquad \begin{aligned} {}^{C}\mathscr{D}_{t}^{\alpha} S &= (r-\mu)S - \omega_{1}S^{2} - (\omega_{2}+\beta)SI + \eta I, \\ {}^{C}\mathscr{D}_{t}^{\alpha} I &= (\beta - \omega_{4})SI - \omega_{3}I^{2} - (\eta+\mu)I. \end{aligned}$$

Since the given process above makes the dimension of time at the left-hand side become t^{α}, some parameters need to be rescaled so that there are no differences between the time's dimensions at the left-hand side with the right-hand side of model (5). By applying time rescale to some parameters, we have the model as follows.

$$(6) \qquad \begin{aligned} {}^{C}\mathscr{D}_{t}^{\alpha} S &= (r^{\alpha} - \mu^{\alpha})S - \omega_{1}^{\alpha}S^{2} - (\omega_{2}^{\alpha}+\beta^{\alpha})SI + \eta^{\alpha}I, \\ {}^{C}\mathscr{D}_{t}^{\alpha} I &= (\beta^{\alpha} - \omega_{4}^{\alpha})SI - \omega_{3}^{\alpha}I^{2} - (\eta^{\alpha}+\mu^{\alpha})I. \end{aligned}$$

Let $r^{\alpha} = \hat{r}$, $\mu^{\alpha} = \hat{\mu}$, $\omega_{1}^{\alpha} = \hat{\omega}_{1}$, $\omega_{2}^{\alpha} = \hat{\omega}_{2}$, $\omega_{3}^{\alpha} = \hat{\omega}_{3}$, $\omega_{4}^{\alpha} = \hat{\omega}_{4}$, $\beta^{\alpha} = \hat{\beta}$, and $\eta^{\alpha} = \hat{\eta}$. Thus, we acquire

$$(7) \qquad \begin{aligned} {}^{C}\mathscr{D}_{t}^{\alpha} S &= (\hat{r}-\hat{\mu})S - \hat{\omega}_{1}S^{2} - (\hat{\omega}_{2}+\hat{\beta})SI + \hat{\eta}I, \\ {}^{C}\mathscr{D}_{t}^{\alpha} I &= (\hat{\beta} - \hat{\omega}_{4})SI - \hat{\omega}_{3}I^{2} - (\hat{\eta}+\hat{\mu})I. \end{aligned}$$

For simplicity, by dropping $\hat{\ }$ for each parameter, we obtain the final model as follows.

$$
^{C}\mathscr{D}_{t}^{\alpha}S = (r-\mu)S - \omega_{1}S^{2} - (\omega_{2}+\beta)SI + \eta I = F_{1}(N(t)),
$$

(8)

$$
^{C}\mathscr{D}_{t}^{\alpha}I = (\beta-\omega_{4})SI - \omega_{3}I^{2} - (\eta+\mu)I = F_{2}(N(t)).
$$

Equation (8) is the final proposed model in this paper. Although model (8) seems classic and simple, this model will be powerful to solve and investigate the existence of a closed population in a certain area without any outside intervention. Our literature review also shows that the model (8) has heretofore never been studied. Now, the basic properties of model (8) such as the existence uniqueness, non-negativity, and boundedness are investigated to confirm its biological validity.

2.2. Existence and Uniqueness. In this subsection, we will show that the model (8) has a unique solution. A similar manner given by [37] is used. Thus, the following theorem is presented to show the existence and uniqueness of the solution of model (8).

Theorem 1. *The model* (8) *with initial condition* $S(0) = S_{0} \geq 0$ *and* $I(0) = I_{0} \geq 0$ *has a unique solution.*

Proof. Consider model (8) with positive initial condition with $F : [0,\infty) \to \mathbb{R}^{2}$ where $F(N) = (F_{1}(N),F_{2}(N))$, $N \equiv N(t)$ and $\theta \equiv \left\{(S,I) \in \mathbb{R}_{+}^{2} : \max\left\{|S|,|I|\right\} \leq M\right\}$ for sufficiently large M. Then, for any $N = (S,I)$ and $\bar{N} = (\bar{S},\bar{I})$, $N,\bar{N} \in \theta$, we have

$$
\|F(N) - F(\bar{N})\|
$$

$$
= |F_{1}(N) - F_{1}(\bar{N})| + |F_{2}(N) - F_{2}(\bar{N})|
$$

$$
= \left|\left[(r-\mu)S - \omega_{1}S^{2} - (\omega_{2}+\beta)SI + \eta I\right] - \left[(r-\mu)\bar{S} - \omega_{1}\bar{S}^{2} - (\omega_{2}+\beta)\bar{S}\bar{I} + \eta\bar{I}\right]\right| +
$$

$$
\left|\left[(\beta-\omega_{4})SI - \omega_{3}I^{2} - (\eta+\mu)I\right] - \left[(\beta-\omega_{4})\bar{S}\bar{I} - \omega_{3}\bar{I}^{2} - (\eta+\mu)\bar{I}\right]\right|
$$

$$
\leq (r+\mu)\left|S-\bar{S}\right| + \omega_{1}\left|S^{2}-\bar{S}^{2}\right| + (\omega_{2}+\beta)\left|SI-\bar{S}\bar{I}\right| + \eta\left|I-\bar{I}\right| + (\beta+\omega_{4})\left|SI-\bar{S}\bar{I}\right|
$$

$$
+ \omega_{3}\left|I^{2}-\bar{I}^{2}\right| + (\eta+\mu)\left|I-\bar{I}\right|
$$

$$
= (r+\mu)\left|S-\bar{S}\right| + \omega_{1}\left|(S+\bar{S})(S-\bar{S})\right| + (\omega_{2}+\omega_{4}+2\beta)\left|I(S-\bar{S}) + \bar{S}(I-\bar{I})\right|
$$

$$
+ (2\eta+\mu)\left|I-\bar{I}\right| + \omega_{3}\left|(I+\bar{I})(I-\bar{I})\right|
$$

$$\leq (r+\mu)\left|S-\bar{S}\right| + 2\omega_1 M\left|S-\bar{S}\right| + (\omega_2 + \omega_4 + 2\beta)M\left|S-\bar{S}\right|$$

$$+ (\omega_2 + \omega_4 + 2\beta)M\left|I-\bar{I}\right| + (2\eta+\mu)\left|I-\bar{I}\right| + 2\omega_3 M\left|I-\bar{I}\right|$$

$$= \left[(r+\mu) + 2\omega_1 M + (\omega_2 + \omega_4 + 2\beta)M\right]\left|S-\bar{S}\right|$$

$$+ \left[(\omega_2 + \omega_4 + 2\beta)M + (2\eta+\mu) + 2\omega_3 M\right]\left|I-\bar{I}\right|$$

$$\leq L\|N-\bar{N}\|,$$

where $L = (\omega_2 + \omega_4 + 2\beta)M + \mu + \max\{r + 2\omega_1 M, 2(\eta + \omega_3 M)\}$. Therefore, $F(N)$ stisfies the Lipschitz condition. Obeying Lemma 5 in [38], we conclude that model (8) with positive initial condition has a unique solution. $\qquad\square$

2.3. Non-negativity and Boundedness. The non-negativity and boundedness properties of the solutions of the model (8) are given in the following theorem.

Theorem 2. *All solution of the model* (8), *which start in* $\mathbb{R}_+^2 :=$ $\left\{(S,I)\,|\,S \geq 0,\ I \geq 0, (S,I) \in \mathbb{R}^2\right\}$ *are uniformly bounded and non-negative.*

Proof. To prove the boundedness of the solutions of the model (8), the same approach of [38] is adopted. Let consider the function $N = S + I$. Then,

$$^{C}\mathscr{D}_t^\alpha N = {}^{C}\mathscr{D}_t^\alpha S + {}^{C}\mathscr{D}_t^\alpha I$$

$$= (r-\mu)S - \omega_1 S^2 - (\omega_2 + \beta)SI + \eta I + (\beta - \omega_4)SI - \omega_3 I^2 - (\eta+\mu)I$$

$$= (r-\mu)S - \omega_1 S^2 - (\omega_2 + \omega_4)SI - \omega_3 I^2 - \mu I.$$

Hence, for each $\mu > 0$,

$$^{C}\mathscr{D}_t^\alpha N + \mu N = (r-\mu)S - \omega_1 S^2 - (\omega_2 + \omega_4)SI - \omega_3 I^2 - \mu I + \mu S + \mu I$$

$$= rS - \omega_1 S^2 - (\omega_2 + \omega_4)SI - \omega_3 I^2$$

$$= -\omega_1\left(S - \frac{r}{2\omega_1}\right)^2 + \frac{r^2}{4\omega_1} - (\omega_2 + \omega_4)SI - \omega_3 I^2$$

$$\leq \frac{r^2}{4\omega_1}$$

By using the comparison theorem in [39], we obtain $N(t) \leq N(0)E_\alpha(-\mu t^\alpha) + \frac{r^2}{4\omega_1}t^\alpha E_{\alpha,\alpha+1}(-\mu t^\alpha)$, where E_α and $E_{\alpha,\alpha+1}$ is the Mittag-Leffler function with one and two parameters. According to Lemma 5 and Corollary 6 in [39], we have $N(t) \leq \frac{r^2}{4\mu\omega_1}$, as $t \to \infty$. Therefore, all solutions of model (8) starting in $\mathbb{R}_+^2$ are uniformly bounded in the region Φ, where $\Phi = \left\{ (S,I) \in \mathbb{R}_+^2 : S+I \leq \frac{r^2}{4\mu\omega_1} + \varepsilon, \ \varepsilon > 0 \right\}$ Next, we prove that all solutions of model (8) are non-negative. By model (8), we have $^C\mathscr{D}_t^\alpha S|_{S=0} = \eta I \geq 0$ and $^C\mathscr{D}_t^\alpha I|_{I=0} = 0 \geq 0$. Based on Lemmas 5 and 6 in [40], we conclude that the solutions of model (8) are non-negative. $\qquad\square$

3. ANALYTICAL RESULTS

In this section, the dynamics of model (8) are shown analytically including the existence of equilibrium points, and their local and global stability.

3.1. Existence of Equilibrium Points.
To find the equilibrium points of model (8), we must have

$$(9) \qquad [(r-\mu) - \omega_1 S - (\omega_2 + \beta)I]S + \eta I = 0,$$

$$(10) \qquad [(\beta - \omega_4)S - \omega_3 I - (\eta + \mu)]I = 0.$$

If $I = 0$ is substituted to (9), we obtain

$$(11) \qquad [(r-\mu) - \omega_1 S]S = 0.$$

From eq. (11), we get $S = 0$ and $S = \frac{r-\mu}{\omega_1}$. Thus, we have two equilibrium points here namely $\mathscr{E}_0 = (0,0)$, and $\mathscr{E}_A = \left(\frac{r-\mu}{\omega_1}, 0 \right)$. The equilibrium point $\mathscr{E}_0$ is called the origin point which represents the extinction of both susceptible and infected populations. Since $\mathscr{E}_0 \in \mathbb{R}_+^2$, this equilibrium point always exists. Furthermore, the equilibrium point $\mathscr{E}_A$ is called the disease-free equilibrium point (DFEP) which describes the condition where the infectious disease does not exist anymore in the population. According to the biological condition, it is natural that the birth rate r is greater than its death rate μ. By assuming $r > \mu$, the origin point $\mathscr{E}_A \in \mathbb{R}_+^2$ also always exists. By simple calculation, we also obtain the basic reproduction number $\mathscr{R}_0$ given by

$$(12) \qquad \mathscr{R}_0 = \frac{(r-\mu)\beta}{(r-\mu)\omega_4 + (\eta+\mu)\omega_1}.$$

The basic reproduction number is utilized to show the dynamical behavior of each equilibrium point and to describe whether the infectious disease becomes endemic or not. Since $r > \mu$, the value of $\mathscr{R}_0$ is always positive. Now, let's concern the eq. (9) and (10). By solving eq. (10), we attain

$$(13) \qquad\qquad S = \frac{\omega_3 I + (\eta + \mu)}{\beta - \omega_4}.$$

If we substitute eq. (13) to (9), the following polynomial equation holds.

$$(14) \qquad\qquad k_1 I^2 + k_2 I + k_3 = 0,$$

where

$$k_1 = ((\beta - \omega_4)(\beta + \omega_2) + \omega_1 \omega_3)\omega_3,$$

$$k_2 = (\beta - \omega_4)((\beta + \omega_2)\mu + (\omega_2 + \omega_4)\eta - (r - \mu)\omega_3) + 2(\eta + \mu)\omega_1 \omega_3,$$

$$k_3 = \frac{(1 - \mathscr{R}_0)(r - \mu)(\eta + \mu)\beta}{\mathscr{R}_0}.$$

Therefore, we acquire the endemic point (EEP)

$$(15) \qquad\qquad \mathscr{E}_I = \left(\frac{\omega_3 \bar{\gamma} + (\eta + \mu)}{\beta - \omega_4}, \bar{\gamma} \right),$$

where $\bar{\gamma}$ is the positive root of polynomial equation (14). From (15), we find that $\beta > \omega_4$ must be fulfilled so that $\mathscr{E}_I \in \mathbb{R}_+^2$. Moreover, EEP exists if $\bar{\gamma} > 0$. From eq. (14), we have k_1 is always positive. Thus, the value of the $\bar{\gamma}$ depends on k_2 and k_3. Furthermore, eq. (14) has real number roots if $k_2^2 \geq 4k_1 k_3$. By applying simple algebra, if $k_3 > 0$ and $k_2 < 0$ then we have two positive roots of eq. (14), if $k_3 > 0$ and $k_2 > 0$ then we do not have any positive roots of eq. (14), and if $k_3 < 0$ then we have a positive root of eq. (14). Finally, we have the following theorem.

Theorem 3. *Let $\beta > \omega_4$. The existence of EEP $\mathscr{E}_I$ is shown by the following statement.*

   (i) If $k_2^2 < 4k_1 k_3$ then $\mathscr{E}_I$ does not exist.

   (ii) If $k_2^2 = 4k_1 k_3$ and

      (ii.i) if $k_2 > 0$ then $\mathscr{E}_I$ does not exist.

      (ii.ii) if $k_2 < 0$ then $\mathscr{E}_I$ exists and unique.

   (iii) If $k_2^2 > 4k_1 k_3$ and

    (iii.i) if $k_3 > 0$ and $k_2 < 0$ then we have a pair of $\mathscr{E}_I$.

    (iii.ii) if $k_3 > 0$ and $k_2 > 0$ then $\mathscr{E}_I$ does not exist.

    (iii.iii) if $k_3 < 0$ then $\mathscr{E}_I$ exists and unique.

Denote that $k_2^2 > 4k_1 k_3$ is always satisfied and $k_3 < 0$ for $\mathscr{R}_0 > 1$, then the following lemma holds.

Lemma 4. *EEP $\mathscr{E}_I$ exists and unique if $\mathscr{R}_0 > 1$.*

3.2. Local Dynamics. The local dynamics of model (8) are obtained by applying the Matignon condition which is defined as follows.

Theorem 5. *[Matignon condition [36]] An equilibrium point $\vec{x}^*$ is locally asymptotically stable (LAS) if all eigenvalues λ_j of the Jacobian matrix $J = \frac{\partial \vec{f}}{\partial \vec{x}}$ at $\vec{x}^*$ satisfy $\left| \arg(\lambda_j) \right| > \frac{\alpha \pi}{2}$. If there exists at least one eigenvalue satisfy $\left| \arg(\lambda_k) \right| > \frac{\alpha \pi}{2}$ while $\left| \arg(\lambda_l) \right| < \frac{\alpha \pi}{2}$, $k \neq l$, then $\vec{x}^*$ is a saddle-point.*

Therefore, to study the local dynamics of model (8), we first compute its Jacobian matrix at the point (S,I) which gives

$$(16) \qquad \mathscr{J}(S,I) = \begin{bmatrix} (r-\mu) - 2\omega_1 S - (\omega_2+\beta)I & -(\omega_2+\beta)S + \eta \\ (\beta-\omega_4)I & (\beta-\omega_4)S - 2\omega_3 I - (\eta+\mu) \end{bmatrix}.$$

Obeying Theorem 5 and using Jacobian matrix (16), we discuss the local stability for each equilibrium point in the next subsection.

3.3. Dynamical behavior around $\mathscr{E}_0$. LAS condition of $\mathscr{E}_0$ is obtained by identifying the eigenvalues of the Jacobian matrix (16) at the point $(S,I) = (0,0)$. We receive

$$\mathscr{J}(S,I)|_{\mathscr{E}_0} = \begin{bmatrix} r-\mu & \eta \\ 0 & -(\eta+\mu) \end{bmatrix}.$$

Therefore, we have $\lambda_1 = r-\mu$ and $\lambda_2 = -(\eta+\mu)$. Since $r > \mu$ and $\lambda_2 < 0$, we have $\left| \arg(\lambda_1) \right| = 0 < \frac{\alpha \pi}{2}$ and $\left| \arg(\lambda_2) \right| = \pi > \frac{\alpha \pi}{2}$. According to Theorem 5, the following theorem holds.

Theorem 6. *The origin point $\mathscr{E}_0$ is always a saddle point.*

3.4. Dynamical behavior around $\mathcal{E}_A$. For $(x,y) = \left(\frac{r-\mu}{\omega_1},0\right)$, the Jacobian matrix (16) becomes

$$\mathscr{J}(S,I)\big|_{\mathcal{E}_A} = \begin{bmatrix} -(r-\mu) & \eta - \frac{(\omega_2+\beta)(r-\mu)}{\omega_1} \\ 0 & \frac{(\mathscr{R}_0-1)(r-\mu)\beta}{\omega_1\mathscr{R}_0} \end{bmatrix},$$

which gives a pair of eigenvalues $\lambda_1 = -(r-\mu)$ and $\lambda_2 = \frac{(\mathscr{R}_0-1)(r-\mu)\beta}{\omega_1\mathscr{R}_0}$. Denote $|\arg(\lambda_2)| = \pi > \frac{\alpha\pi}{2}$ as the impact of $\lambda_1 < 0$. Hence, the sign of λ_2 takes the role in describing local dynamics around $\mathcal{E}_A$. To obtain $|\arg(\lambda_2)| = \pi > \frac{\alpha\pi}{2}$, we need $\lambda_2 < 0$ which is fulfilled if $\mathscr{R}_0 < 1$. If $\mathscr{R}_0 > 1$ then $|\arg(\lambda_2)| = 0 < \frac{\alpha\pi}{2}$. Following the Matignon condition given in Theorem 5, the following theorem is successfully attained.

Theorem 7. *If $\mathscr{R}_0 < 1$ then $\mathcal{E}_A$ is LAS and a saddle point if $\mathscr{R}_0 > 1$.*

3.5. Dynamical behavior around $\mathcal{E}_I$. To identify the local stability of $\mathcal{E}_I$, we first compute the Jacobian matrix (16) evaluated at $\mathcal{E}_I$. We generate

$$(17) \qquad \mathscr{J}(S,I)\big|_{\mathcal{E}_I} = \begin{bmatrix} -\left[\frac{(\omega_3\bar{\gamma}+\eta+\mu)\omega_1}{\beta-\omega_4} + \frac{(\beta-\omega_4)\eta\bar{\gamma}}{\omega_3\bar{\gamma}+\eta+\mu}\right] & -\frac{(\omega_2+\beta)(\omega_3\bar{\gamma}+\eta+\mu)}{\beta-\omega_4} + \eta \\ (\beta-\omega_4)\bar{\gamma} & -\omega_3\bar{\gamma} \end{bmatrix}.$$

The eigenvalues of (17) are given by $\lambda_1 = \frac{1}{2}\left(\xi_1 + \sqrt{\xi_1^2 - 4\xi_2}\right)$ and $\lambda_2 = \frac{1}{2}\left(\xi_1 - \sqrt{\xi_1^2 - 4\xi_2}\right)$ where

$$\xi_1 = -\left[\frac{(\omega_3\bar{\gamma}+\eta+\mu)\omega_1}{\beta-\omega_4} + \frac{(\beta-\omega_4)\eta\bar{\gamma}}{\omega_3\bar{\gamma}+\eta+\mu} + \omega_3\bar{\gamma}\right],$$

$$\xi_2 = \left[\left(\frac{\omega_1\omega_3}{\beta-\omega_4} + \omega_2 + \beta\right)(\omega_3\bar{\gamma}+\eta+\mu) + \left(\frac{\omega_3\bar{\gamma}}{\omega_3\bar{\gamma}+\eta+\mu} + 1\right)(\beta-\omega_4)\eta\right]\bar{\gamma}.$$

It is easy to proof that $\xi_1 < 0$ and $\xi_2 > 0$ since $\beta > \omega_4$ becomes the existence condition. As the impact, $|\arg(\lambda_i)| > \frac{\alpha\pi}{2}$, $i = 1,2$ and hence the LAS always hold for EEP. Thus, the following theorem holds.

Theorem 8. *EEP $\mathcal{E}_I$ is always LAS.*

3.6. Global Dynamics. In this subsection, the global dynamics of model (8) are studied. The biological conditions of equilibrium points are investigated so that those points are globally asymptotically stable (GAS). Since the origin is always a saddle point, we focus on studying GAS conditions for DFEP and EEP. The next two theorems are given for the global dynamics.

Theorem 9. *DFEP $\mathscr{E}_A$ is GAS if $\omega_1 > \frac{(\omega_2+\beta)r}{\mu}$.*

Proof. We define a positive Lyapunov function as follows.

$$(18) \qquad \mathscr{V}_A(S,I) = \left(S - \frac{r-\mu}{\omega_1} - \frac{r-\mu}{\omega_1} \ln \frac{\omega_1 S}{r-\mu} \right) + I.$$

If we calculate the Caputo fractional derivative of $\mathscr{V}_A(S,I)$ along the solution of model (8) and use Lemma 3.1 in [41], we get

$$
{}^C\mathscr{D}_t^\alpha \mathscr{V}_A(S,I)
$$

$$
= \left(\frac{S - \frac{r-\mu}{\omega_1}}{S} \right) {}^C\mathscr{D}_t^\alpha S + {}^C\mathscr{D}_t^\alpha I
$$

$$
= -\omega_1 \left(S - \frac{r-\mu}{\omega_1} \right)^2 + \frac{(r-\mu)(\omega_2+\beta)I}{\omega_1} - \frac{(r-\mu)\eta I}{\omega_1 S} - (\omega_2+\omega_4)SI - \omega_3 I^2 - \mu I
$$

$$
\leq -\omega_1 \left(S - \frac{r-\mu}{\omega_1} \right)^2 - \left(\mu - \frac{(\omega_2+\beta)r}{\omega_1} \right) I
$$

Since $\omega_1 > \frac{(\omega_2+\beta)r}{\mu}$, we have ${}^C\mathscr{D}_t^\alpha \mathscr{V}_A(S,I) \leq 0$ for all $(S,I) \in \mathbb{R}_+^2$, and ${}^C\mathscr{D}_t^\alpha \mathscr{V}_A(S,I) = 0$ only when $(S,I) = \left(\frac{r-\mu}{\omega_1}, 0 \right)$. This means that the singleton $\{\mathscr{E}_A\}$ is the only invariant set where ${}^C\mathscr{D}_t^\alpha \mathscr{V}_A(S,I) = 0$. By Lemma 4.6 in [42], we can conclude that every solution of model (8) tends to DFEP $\mathscr{E}_A$.

$\square$

Theorem 10. *EEP $\mathscr{E}_I$ is GAS if $\frac{\omega_2}{2} + \frac{\omega_4}{2} + \frac{\eta}{2\vartheta} < \min\{\omega_1, \omega_3\}$.*

Proof. We first define $\vartheta = \frac{\omega_3 \bar{\gamma} + (\eta + \mu)}{\beta - \omega_4}$ and hence $\mathscr{E}_I = (\vartheta, \bar{\gamma})$. Now, a positive Lyapunov function is presented as follows.
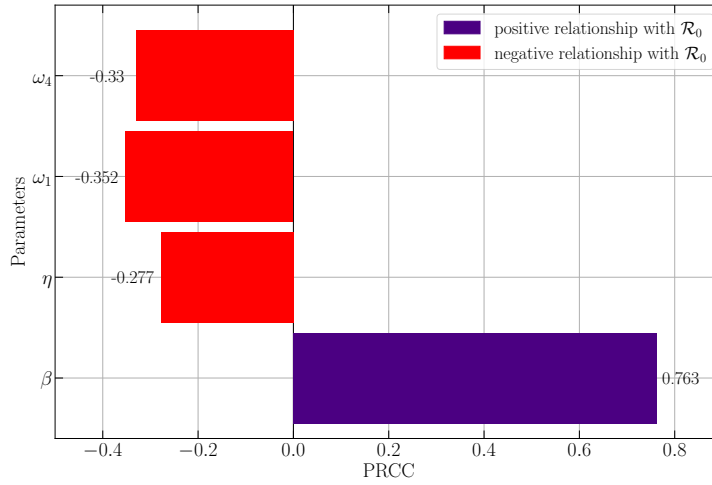
$$(19) \qquad \mathscr{V}_I(S,I) = \left(S - \vartheta - \vartheta \ln \frac{S}{\varphi} \right) + \left(I - \bar{\gamma} - \bar{\gamma} \ln \frac{S}{\bar{\gamma}} \right)$$

Following Lemma 3.1 in [41], we reach

$$
{}^C\mathscr{D}_t^\alpha \mathscr{V}_I(S,I)
$$

$$
= \left(\frac{S - \vartheta}{S} \right) {}^C\mathscr{D}_t^\alpha S + \left(\frac{I - \bar{\gamma}}{I} \right) {}^C\mathscr{D}_t^\alpha I
$$

$$
= (S - S^*) \left((r-\mu) - \omega_1 S - (\omega_2+\beta)I + \frac{\eta I}{S} \right) + (I - \bar{\gamma})\left((\beta - \omega_4)S - \omega_3 I - (\eta + \mu) \right)
$$

$$= -\omega_1 (S - \vartheta)^2 - \omega_3 (I - \bar{\gamma})^2 - (\omega_2 + \omega_4)(S - S^*)(I - \bar{\gamma})$$

$$\leq -\left(\omega_1 - \left(\frac{\omega_2}{2} + \frac{\omega_4}{2} + \frac{\eta}{2\vartheta}\right)\right)(S - \vartheta)^2 - \left(\omega_3 - \left(\frac{\omega_2}{2} + \frac{\omega_4}{2} + \frac{\eta}{2\vartheta}\right)\right)(I - \bar{\gamma})^2$$

Denote that $^C\mathscr{D}_t^\alpha \mathscr{V}_I(S,I) \leq 0$ for all $(S,I) \in \mathbb{R}_+^2$ as a result of $\frac{\omega_2}{2} + \frac{\omega_4}{2} + \frac{\eta}{2\vartheta} < \min\{\omega_1, \omega_3\}$. We also have that $^C\mathscr{D}_t^\alpha \mathscr{V}_I(S,I) = 0$ only when $(S,I) = (\vartheta, \bar{\gamma})$. Therefore, the singleton $\{\mathscr{E}_I\}$ is the only invariant set where $^C\mathscr{D}_t^\alpha \mathscr{V}_I(S,I) = 0$. Obeying Lemma 4.6 in [42], every solution of model (8) tends to EEP $\mathscr{E}_I$. $\qquad\square$

FIGURE 2. PRCC results for the parameters of $\mathscr{R}_0$

(A) Contour plot on $(\omega_1, \omega_4)-$ plane

(B) Contour plot on $(\beta, \eta)-$ plane
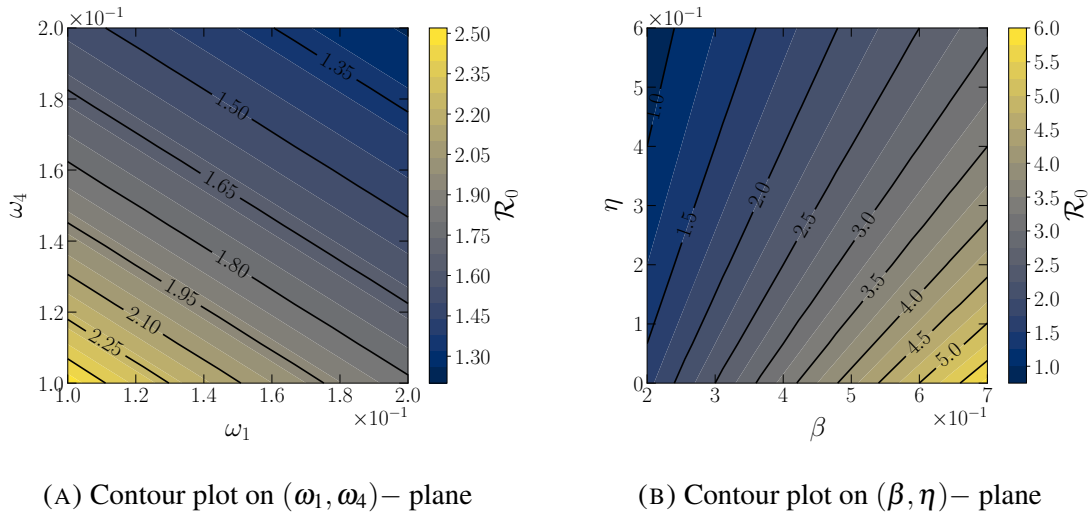
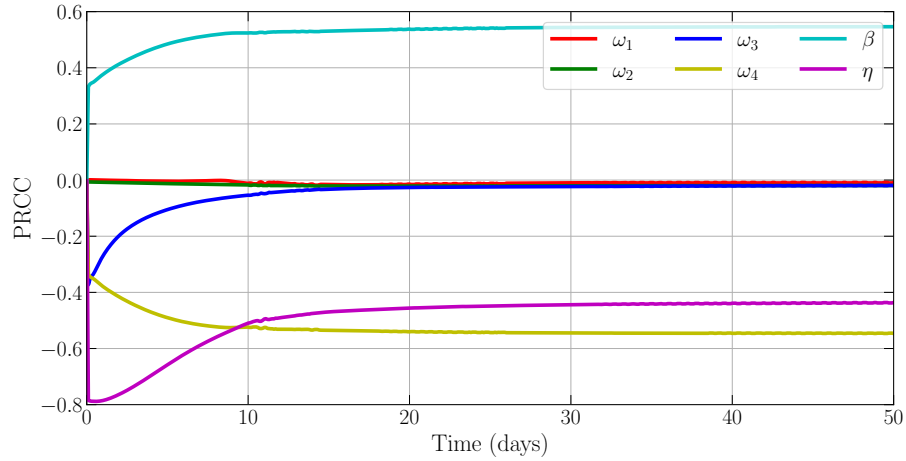FIGURE 3. Contour plots for the parameters respect to $\mathscr{R}_0$

FIGURE 4. PRCC results for the parameters of $I(t)$

TABLE 1. PRCC results in respect to the population density of infected class

Parameter	Description	PRCC	Rank	Relationship with $I(t)$
ω_1	The death rate of susceptible population due to the intraspecific competition	-0.00851	6	Negative relationship
ω_2	The death rate of susceptible population due to the interspecific competition	-0.01938	5	Negative relationship
ω_3	The death rate of infected population due to the intraspecific competition	-0.01990	4	Negative relationship
ω_4	The death rate of infected population due to the interspecific competition	-0.54635	1	Negative relationship
β	The infection rate	0.54631	2	Positive relationship
η	The recovery rate	-0.43606	3	Negative relationship
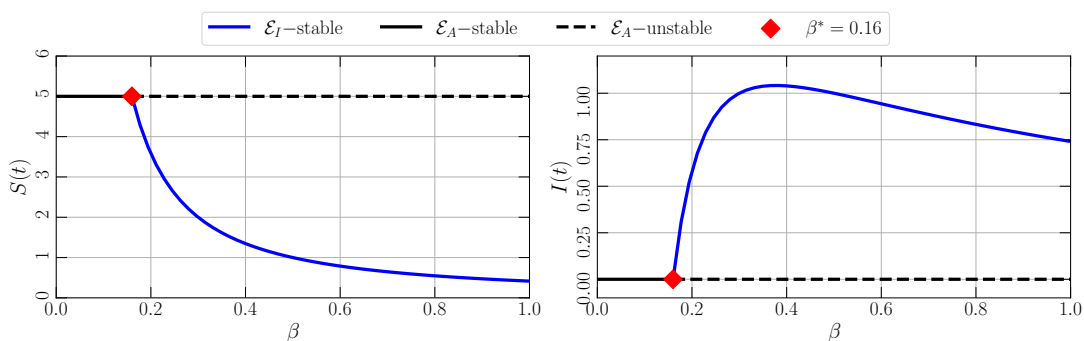
(A) Bifurcation diagram driven by β in interval $0 \leq \beta \leq 1$
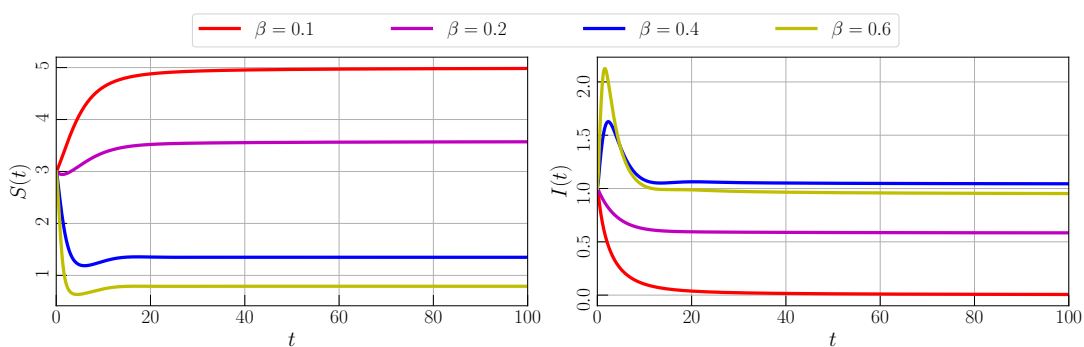
(B) Time-series for $\beta = 0.1, 0.2, 0.4$, and 0.6

FIGURE 5. Bifurcation diagram and times-series of model (8) driven by the infection rate (β) with parameter values given by eq. (20)
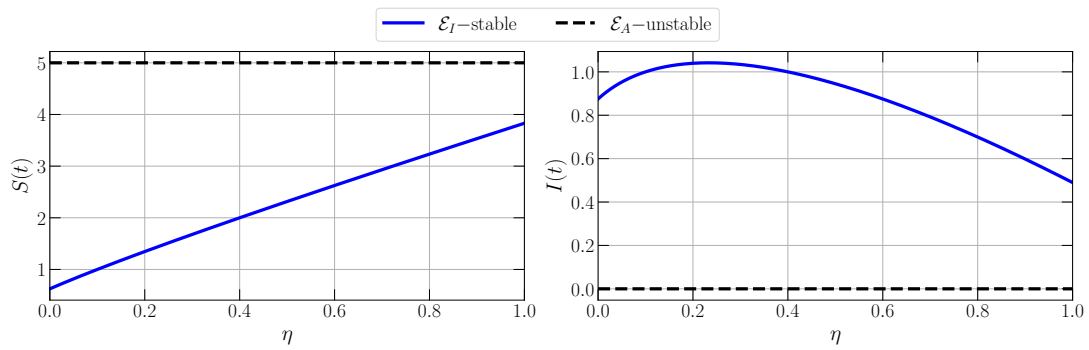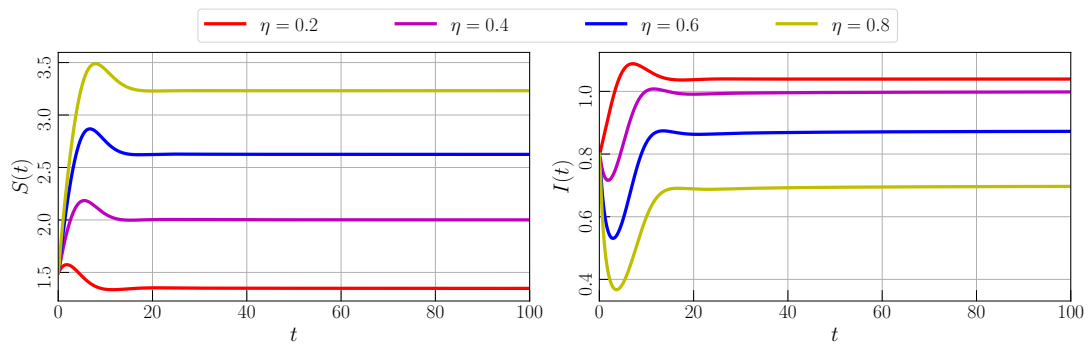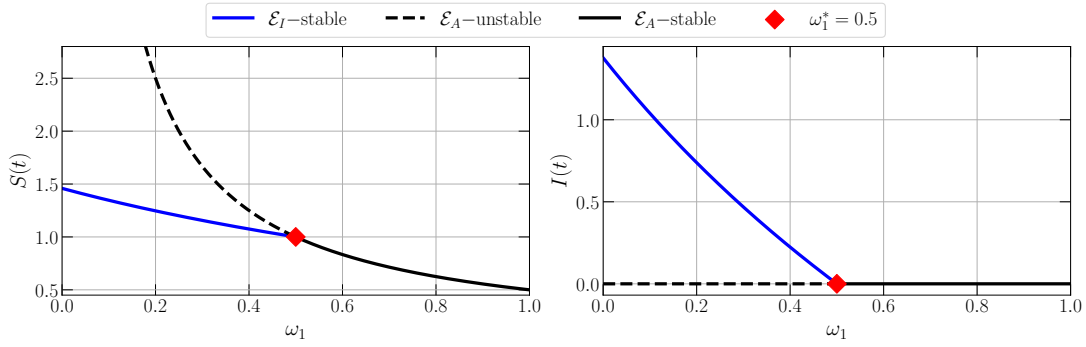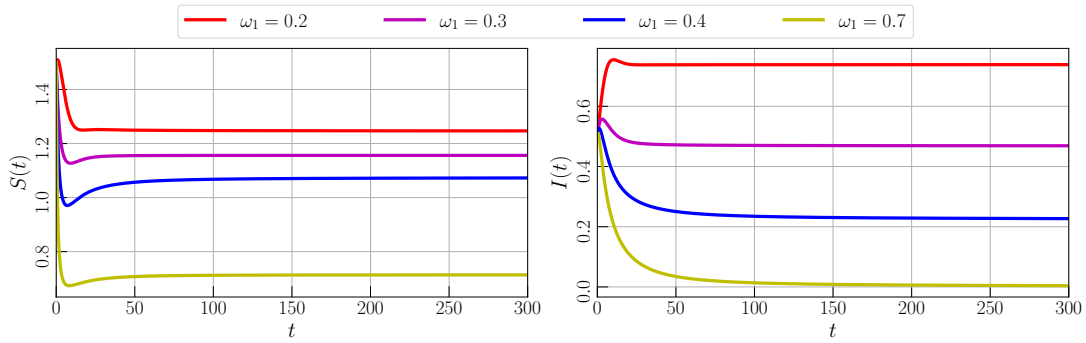
(A) Bifurcation diagram driven by η in interval $0 \leq \eta \leq 1$

(B) Time-series for $\eta = 0.2, 0.4, 0.6,$ and 0.8

FIGURE 6. Bifurcation diagram and times-series of model (8) driven by the recovery rate (η) with parameter values given by eq. (20)

(A) Bifurcation diagram driven by ω_1 in interval $0 \leq \omega_1 \leq 1$

(B) Time-series for $\omega_1 = 0.2, 0.3, 0.4$, and 0.7

FIGURE 7. Bifurcation diagram and times-series of model (8) driven by the death rate of susceptible population due to intraspecific competition (ω_1) with parameter values given by eq. (20)
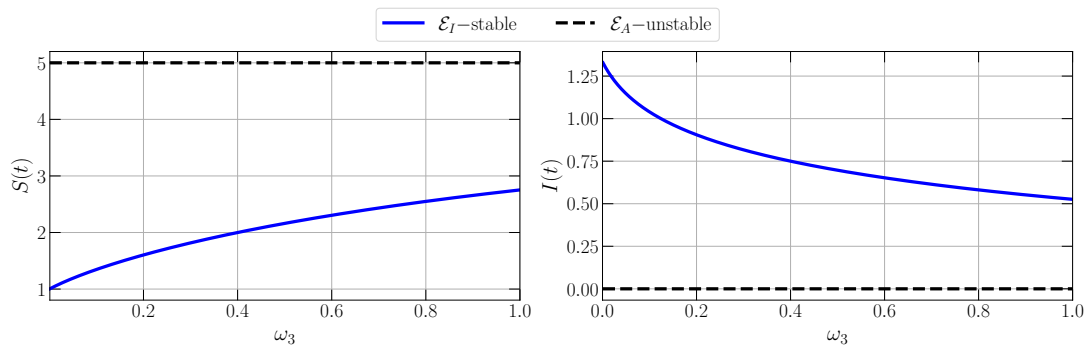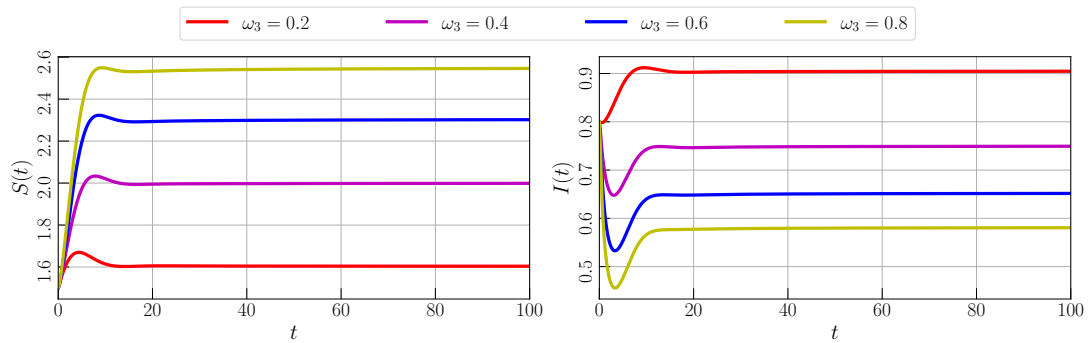
(A) Bifurcation diagram driven by ω_3 in interval $0 \leq \omega_3 \leq 1$

(B) Time-series for $\omega_3 = 0.2, 0.4, 0.6,$ and 0.8

FIGURE 8. Bifurcation diagram and times-series of model (8) driven by the death rate of infected population due to intraspecific competition (ω_3) with parameter values given by eq. (20)

(A) Bifurcation diagram driven by ω_2 in interval $0 \leq \omega_2 \leq 1$

(B) Time-series for $\omega_2 = 0.2, 0.4, 0.6,$ and 0.8

FIGURE 9. Bifurcation diagram and times-series of model (8) driven by the death rate of susceptible population due to interspecific competition (ω_2) with parameter values given by eq. (20)
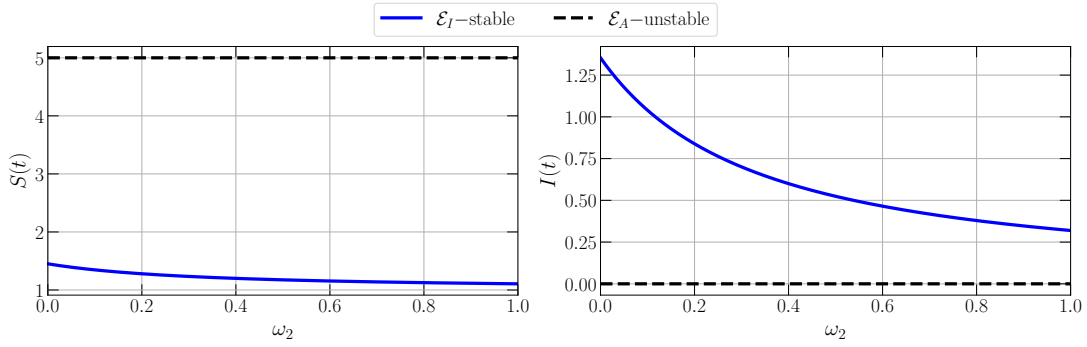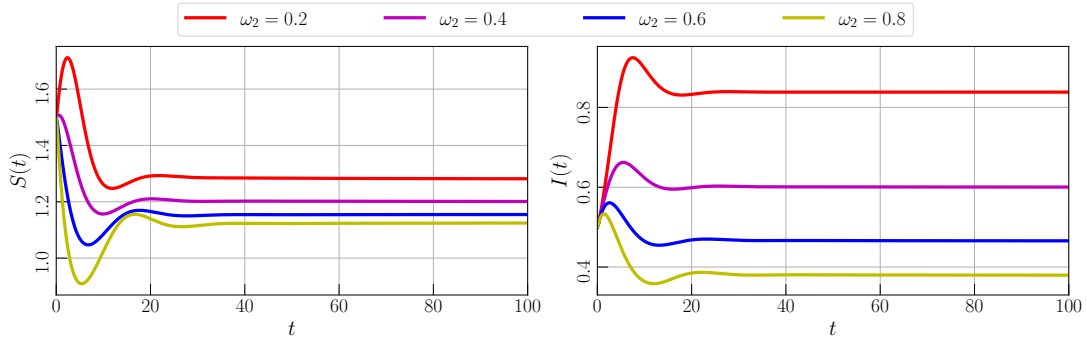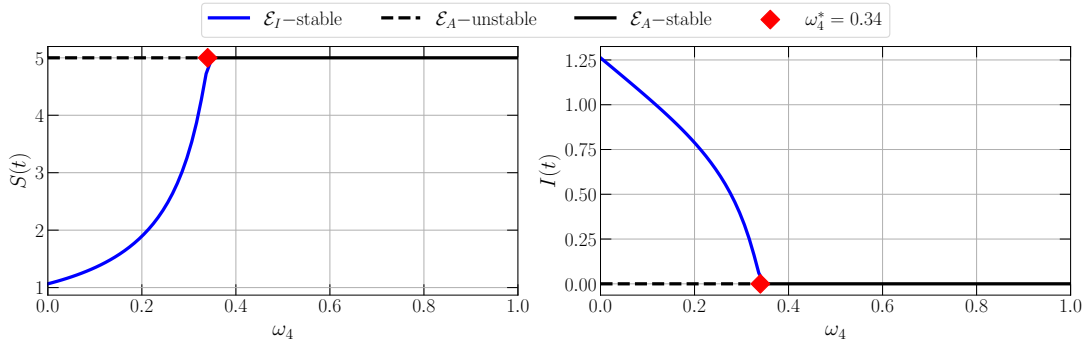
(A) Bifurcation diagram driven by ω_4 in interval $0 \leq \omega_4 \leq 1$
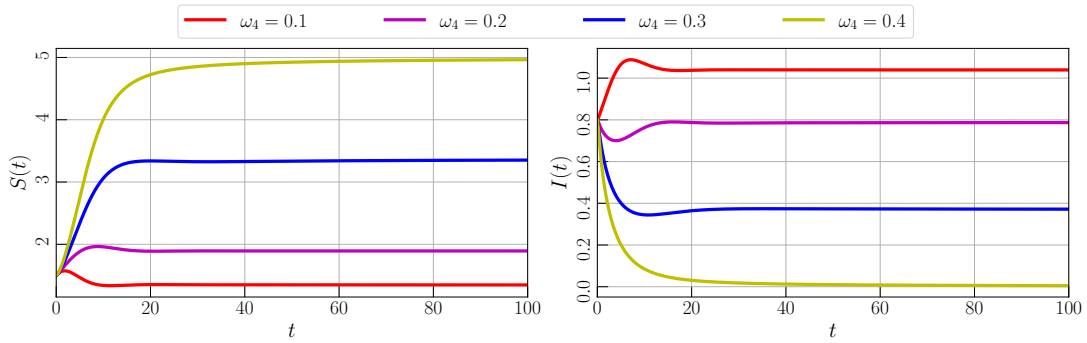
(B) Time-series for $\omega_4 = 0.2, 0.4, 0.6$, and 0.8

FIGURE 10. Bifurcation diagram and times-series of model (8) driven by the death rate of infected population due to interspecific competition (ω_4) with parameter values given by eq. (20)

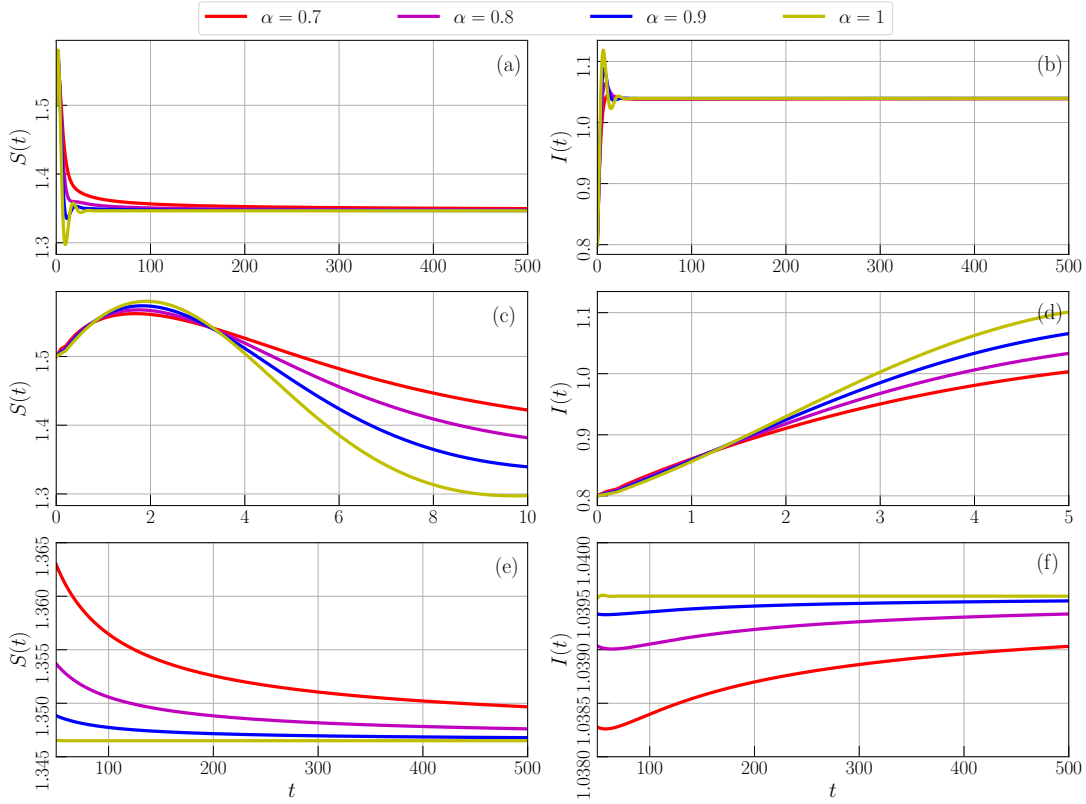FIGURE 11. Time series of model (8) with parameter values given by eq. (20) for $\alpha = 0.7, 0.8, 0.9, 1$. **(a,b)** Time-series for $0 \leq t \leq 500$, **(c,d)** Local amplification of (a,b) around $0 \leq t \leq 10$, and **(c,d)** Local amplification of (a,b) around $100 \leq t \leq 500$

4. GLOBAL SENSITIVITY ANALYSIS

In this section, the global sensitivity analysis is studied to investigate the most influential parameters of model (8). Global sensitivity analysis is calculated using Partial Rank Coefficient Correlation (PRCC) [43], where the random data processed in PRCC is generated using Saltelli sampling [44]. Two biological components become the objective function for the PRCC namely the basic reproduction number ($\mathscr{R}_0$) and the population density of infected class ($I(t)$). We first investigate the most influential parameter to the basic reproduction number ($\mathscr{R}_0$). From eq. (12), we acquire that only r, μ, ω_1, ω_4, and η have the influence on the value of $\mathscr{R}_0$. The birth rate and the natural death rate also can be fixed since some cases in the epidemiological model has the values of these parameters. Thus, only β, η, ω_1, and ω_4 will be computed for PRCC. The Figure 2 is given for the results. We have $\beta = 0.763$, $\omega_1 = -0.352$, $\omega_4 = -0.33$, and $\eta = -0.277$ as the coefficient correlation such that the infection rate (β) becomes the most influential parameter to $\mathscr{R}_0$ and followed by ω_1, ω_4, and η, respectively. It shows that the infection rate (β) as the most influential parameter has a positive relationship with the basic reproduction number ($\mathscr{R}_0$) which means that $\mathscr{R}_0$ will significantly increases when β increases. The rest ω_1, ω_4, and η have a negative relationship with $\mathscr{R}_0$ which means that by reducing the value of those parameters, the basic reproduction number ($\mathscr{R}_0$) will increases. To show the impact of these parameters on $\mathscr{R}_0$, the contour plots are also portrayed in Figure 3.

Next, we identify the most influential parameter to the population density of infected class ($I(t)$). Quite similar to previous work, the value of r and μ are fixed but the rest of the parameters are involved to compute PRCC. PRCC values are computed for $0 \leq t \leq 50$ which is considered sufficient enough to see the convergence for each parameter through the PRCC. We portray the PRCC results in Figure 4 while the PRCC values, ranks, and the relationship between each parameter and $I(t)$ are given in Table 1. From those simulations, we conclude that the death rate of infected population due to interspecific competition between susceptible and infected classes (ω_4) become the most influential parameter to the population density ($I(t)$) followed respectively by β, η, ω_3, ω_2, and ω_1. In the next section, the numerical simulations including bifurcation diagram and time-series are presented to show the impact of the infection

rate (β), recovery rate (η), intraspecific competition $(\omega_1$ and $\omega_3)$, and interspecific competition $(\omega_2$ and $\omega_4)$ to the dynamical behaviors of model (8).

5. NUMERICAL SIMULATIONS

In this section, the dynamical behaviors of model (8) including bifurcation diagram and time-series are studied numerically. To obtain the bifurcation diagram and the corresponding time-series of model (8), the predictor-corrector scheme developed by Diethelm et al. is employed [45]. Since the model does not investigate a specific epidemiological case, we use hypothetical parameters for all numerical simulations. we set the parameter values as follows.

(20)

$$r = 0.6, \ \mu = 0.1, \ \omega_1 = 0.1, \ \omega_2 = 0.1, \ \omega_3 = 0.1, \ \omega_4 = 0.1, \ \beta = 0.4, \ \eta = 0.2, \text{ and } \alpha = 0.9$$

We start our work by investigating the impact of infection rate (β) on the dynamics of model (8). The value of β is varied in the interval $0 \leq \beta \leq 1$ and we then compute the numerical solutions. To obtain the bifurcation diagram, we plot the tail of solutions for each β together with the LAS condition of $\mathscr{E}_A$. As result, we obtain a bifurcation diagram as in Figure 5a. When $0 \leq \beta < \beta^*$, $\beta^* = 0.16$, the EEP $\mathscr{E}_I$ does not exist and Theorem 7 is satisfied which means that DFE $\mathscr{E}_A$ is LAS. The solution is convergent to $\mathscr{E}_A$ which indicates the population free from disease. When β passes through β^*, $\mathscr{E}_A$ loses its stability, and unique LAS EEP $\mathscr{E}_I$ occurs in the interior. The infectious disease becomes endemic in the population and still exists for all $t \to \infty$. From the concatenation of those biological circumstances, we conclude that forward bifurcation occurs around $\mathscr{E}_A$ where β is the bifurcation parameter and $\beta = \beta^*$ is the bifurcation point. It is easy to examine that the bifurcation point $\beta = \beta^*$ is equal to $\mathscr{R}_0 = 1$. The dynamical behaviors are maintained for $\beta^* < \beta \leq 1$. To support these conditions, some time series are given in Figure 5b to show the convergence of solutions for different values of β.

Next, the impact of recover rate (η) is studied. A similar numerical scheme as the previous way is applied. To depicts the bifurcation diagram, the parameter is fixed as in eq. (20) and the recovery rate (η) is varied in interval $0 \leq \eta \leq 1$. We have Figure 6a as the result. Denote that the bifurcation does not exist for this interval. Both DFEP and EEP exist with distinct stability. The DFEP $\mathscr{E}_A$ is a saddle point while the EEP $\mathscr{E}_I$ is LAS which confirm the validity of Theorems 6

and 7. We also confirm that the EEP $\mathscr{E}_I$ attains GAS which means that all initial conditions will go right to the EEP and the infectious disease will exist all the time. Although the disease becomes endemic, the numerical simulation shows that the value of η is directly proportional to $S(t)$ and inversely proportional to $I(t)$, see Figure 6b. This means the population density of the infected class can be reduced by increasing the recovery rate (η).

For the next simulation, the impact of intraspecific competition is investigated. The death rate parameters caused by intraspecific competition on susceptible and infected classes (ω_1 and ω_3) are varied in interval $[0,1]$. It is found that forward bifurcation occurs when ω_1 is driven where the bifurcation point is given by $\omega_1^* = 0.5$, see Figure 7a. The population density of both susceptible and infected classes reduces when the death rate of $S(t)$ due to intraspecific competition increases as given by Figure 7b. Particularly, Figure 8a shows that bifurcation does not exists in interval $0 \leq \omega_1 \leq 1$ when ω_1 is varied but the dynamical behaviors show that $S(t)$ increases and $I(t)$ decrease when ω_1 increase. We confirm this condition by giving time-series in Figure 8b.

Now, we study the impact of interspecific competition on the dynamical behaviors of model (8). Both susceptible and infected classes have died due to the existence of interspecific competition given by parameters ω_2 and ω_4. By varying ω_2 and ω_4 in interval $[0,1]$, we obtain Figures 9a and 10a as the bifurcation diagram. We find forward bifurcation driven by ω_4 which does not exist when varying ω_1. This means, the EEP still exists and LAS for $0 \leq< \omega_2 \leq 1$. The EEP will disappear via forward bifurcation and the saddle DFEP becomes LAS when ω_4 crosses $\omega_4^* = 0.34$. This guarantees that the infectious disease may eliminate the disease in population when the death rate of the infected population due to interspecific competition increases as shown in Figure 10b. Although the disease does not disappear when ω_2 is driven, we also can see in Figure 9b that by increasing ω_2, the population density of the infected class will reduce and the susceptible class will increase.

Finally, the impact of memory effect (α) is investigated. The numerical simulation is given by Figure 11. For $\alpha = 0.7, 0.8, 0.9, 1$ and similar initial values, all solution converge to single equilibrium point given by $\mathscr{E}_I \approx (1.3465, 1.0395)$, see Figure 11(a,b). We then plot the local amplification to show the difference of solutions when α is varied. We find that the difference

lies in the convergence rate where for larger values of α, the convergence rate increase and vice versa as shown in Figure 11(e,f). In the beginning, Figure 11(c,d) we show that when α decrease, the population density of the infected class reduce. From a biological point of view, we can say that biological memory has an impact on the density of both susceptible and infected classes.

6. CONCLUSION

The dynamics of a fractional-order SIS-epidemic model with intraspecific and interspecific competition have been studied. The validity of the model has been confirmed analytically by showing the existence, uniqueness, non-negativity, and boundedness of solutions. Three equilibrium points have been obtained namely the origin, the disease-free equilibrium point, and the endemic equilibrium point. Both origin and disease-free equilibrium points always exist while the endemic equilibrium point conditionally exists. The basic reproduction number $\mathscr{R}_0$ has been given which has a relationship with the local stability of the model. If $\mathscr{R}_0 < 1$ then the disease-free equilibrium point is locally asymptotically stable and if $\mathscr{R}_0 > 1$ then the disease-free equilibrium point losses its stability along with the existence of a locally asymptotically stable endemic equilibrium point. The global stability conditions of equilibrium points also have been found. The PRCC has been worked to investigate the most influential parameter. We have successfully shown that the infection rate and the death rate of the infected population due to interspecific competition becomes the most influential parameter for basic reproduction number and the population density of the infected class. We then investigate the impact of several parameters using numerical simulations including the infection rate, the recovery rate, the intraspecific competition, the interspecific competition, and the memory effect on the dynamics of the model. Bifurcation diagrams and time series have been given which show the existence of forward bifurcation, the decrease of susceptible and infected classes, and the decrease of convergence rate caused by the memory effect.

CONFLICT OF INTERESTS

The author(s) declare that there is no conflict of interests.

REFERENCES

[1] H. Cao, H. Wu, X. Wang, Bifurcation analysis of a discrete SIR epidemic model with constant recovery, Adv. Differ. Equ. 2020 (2020), 49. https://doi.org/10.1186/s13662-020-2510-9.

[2] H.W. Hethcote, The mathematics of infectious diseases, SIAM Rev. 42 (2000), 599–653. https://doi.org/10.1137/s0036144500371907.

[3] F. Brauer, Mathematical epidemiology: Past, present, and future, Infect. Dis. Model. 2 (2017), 113–127. https://doi.org/10.1016/j.idm.2017.02.001.

[4] R. Sanft, A. Walter, Exploring mathematical modeling in biology through case studies and experimental activities, Academic Press, London, 2020.

[5] W.O. Kermack, A.G. McKendrick, A contribution to the mathematical theory of epidemics, Proc. R. Soc. Lond. A. 115 (1927), 700–721. https://doi.org/10.1098/rspa.1927.0118.

[6] M. Liu, X. Fu, D. Zhao, Dynamical analysis of an SIS epidemic model with migration and residence time, Int. J. Biomath. 14 (2021), 2150023. https://doi.org/10.1142/s1793524521500236.

[7] X. Liu, K. Zhao, J. Wang, et al. Stability analysis of a SEIQRS epidemic model on the finite scale-free network, Fractals. 30 (2022), 2240054. https://doi.org/10.1142/s0218348x22400540.

[8] M.M. Ojo, O.J. Peter, E.F.D. Goufo, et al. Mathematical model for control of tuberculosis epidemiology, J. Appl. Math. Comput. (2022). https://doi.org/10.1007/s12190-022-01734-x.

[9] I. Darti, A. Suryanto, H. S. Panigoro, et al. Forecasting COVID-19 epidemic in Spain and Italy using a generalized Richards model with quantified uncertainty, Commun. Biomath. Sci. 3 (2022), 90–100. https://doi.org/10.5614/cbms.2020.3.2.1.

[10] M. Lu, C. Xiang, J. Huang, Bogdanov-Takens bifurcation in a SIRS epidemic model with a generalized nonmonotone incidence rate, Discr. Contin. Dyn. Syst. - S. 13 (2020), 3125–3138. https://doi.org/10.3934/dcdss.2020115.

[11] B. Li, C. Qin, X. Wang, Analysis of an SIRS epidemic model with nonlinear incidence and vaccination, Commun. Math. Biol. Neurosci., 2020 (2020), 2. https://doi.org/10.28919/cmbn/4262.

[12] F.F. Eshmatov, U.U. Jamilov, Kh.O. Khudoyberdiev, Discrete time dynamics of a SIRD reinfection model, Int. J. Biomath. (2022). https://doi.org/10.1142/s1793524522501042.

[13] A. Miao, X. Wang, T. Zhang, et al. Dynamical analysis of a stochastic SIS epidemic model with nonlinear incidence rate and double epidemic hypothesis, Adv. Differ. Equ. 2017 (2017), 226. https://doi.org/10.1186/s13662-017-1289-9.

[14] D. Zhao, S. Yuan, H. Liu, Random periodic solution for a stochastic SIS epidemic model with constant population size, Adv. Differ. Equ. 2018 (2018), 64. https://doi.org/10.1186/s13662-018-1511-4.

[15] J. Liu, B. Liu, P. Lv, et al. An eco-epidemiological model with fear effect and hunting cooperation, Chaos Solitons Fractals. 142 (2021), 110494. https://doi.org/10.1016/j.chaos.2020.110494.

[16] S. Kumar, H. Kharbanda, Sensitivity and chaotic dynamics of an eco-epidemiological system with vaccination and migration in prey, Braz. J. Phys. 51 (2021), 986–1006. https://doi.org/10.1007/s13538-021-00862-2.

[17] D. Bhattacharjee, A.J. Kashyap, H.K. Sarmah, et al. Dynamics in a ratio-dependent eco-epidemiological predator-prey model having cross species disease transmission, Commun. Math. Biol. Neurosci. 2021 (2021), 15. https://doi.org/10.28919/cmbn/5302.

[18] S. Jana, M. Mandal, S.K. Nandi, et al. Analysis of a fractional-order SIS epidemic model with saturated treatment, Int. J. Model. Simul. Sci. Comput. 12 (2020), 2150004. https://doi.org/10.1142/s1793962321500045.

[19] A. Lahrouz, H. El Mahjour, A. Settati, et al. Bifurcation from an epidemic model in the presence of memory effects, Int. J. Bifurcation Chaos. 32 (2022), 2250077. https://doi.org/10.1142/s0218127422500778.

[20] E. Bonyah, M.L. Juga, C.W. Chukwu, et al. A fractional order dengue fever model in the context of protected travelers, Alexandria Eng. J. 61 (2022), 927–936. https://doi.org/10.1016/j.aej.2021.04.070.

[21] C. Maji, Dynamical analysis of a fractional-order predator–prey model incorporating a constant prey refuge and nonlinear incident rate, Model. Earth Syst. Environ. 8 (2021), 47–57. https://doi.org/10.1007/s40808-020-01061-9.

[22] H.S. Panigoro, A. Suryanto, W.M. Kusumawinahyu, et al. A Rosenzweig–MacArthur model with continuous threshold harvesting in predator involving fractional derivatives with power law and Mittag–Leffler kernel, Axioms. 9 (2020), 122. https://doi.org/10.3390/axioms9040122.

[23] S. Majee, S. Adak, S. Jana, et al. Complex dynamics of a fractional-order SIR system in the context of COVID-19, J. Appl. Math. Comput. (2022). https://doi.org/10.1007/s12190-021-01681-z.

[24] I. Podlubny, Fractional differential equations: An introduction to fractional derivatives, fractional differential equations, to methods of their solution and some of their applications, Academic Press, San Diego CA, 1999.

[25] M. Caputo, Linear models of dissipation whose q is almost frequency independent–II, Geophys. J. Int. 13 (1967), 529–539. https://doi.org/10.1111/j.1365-246x.1967.tb02303.x.

[26] M. Caputo, M. Fabrizio, A new definition of fractional derivative without singular kernel, Progress Fract. Differ. Appl. 1 (2015), 73–85.

[27] A. Atangana, D. Baleanu, New fractional derivatives with nonlocal and non-singular kernel: Theory and application to heat transfer model, Therm. Sci. 20 (2016), 763–769. https://doi.org/10.2298/TSCI160111018A.

[28] J. Philippa, R. Dench, Infectious diseases of orangutans in their home ranges and in zoos, in: Fowler's Zoo and Wild Animal Medicine Current Therapy, Volume 9, Elsevier, 2019: pp. 565–573. https://doi.org/10.1016/B978-0-323-55228-8.00080-1.

[29] A. Aswad, A. Katzourakis, The first endogenous herpesvirus, identified in the tarsier genome, and novel sequences from primate rhadinoviruses and lymphocryptoviruses, PLoS Genet. 10 (2014), e1004332. https://doi.org/10.1371/journal.pgen.1004332.

[30] B.H. Mulia, S. Mariya, J. Bodgener, et al. Exposure of wild sumatran tiger (panthera tigris sumatrae) to canine distemper virus, J. Wildlife Dis. 57 (2021), 464–466. https://doi.org/10.7589/jwd-d-20-00144.

[31] M. Skoric, V. Mrlik, J. Svobodova, et al. Infection in a female Komodo dragon (Varanus komodoensis) caused by Mycobacterium intracellulare: A case report, Vet. Med. 57 (2012), 163–168.

[32] D. Mukherjee, Role of fear in predator–prey system with intraspecific competition, Math. Computers Simul. 177 (2020), 263–275. https://doi.org/10.1016/j.matcom.2020.04.025.

[33] C. Arancibia-Ibarra, P. Aguirre, J. Flores, et al. Bifurcation analysis of a predator-prey model with predator intraspecific interactions and ratio-dependent functional response, Appl. Math. Comput. 402 (2021), 126152. https://doi.org/10.1016/j.amc.2021.126152.

[34] E. Bodine, A. Yust, Predator-prey Dynamics with Intraspecific Competition and an Allee Effect in the Predator Population, Lett. Biomath. 4 (2017), 23–38. https://doi.org/10.30707/lib4.1bodine.

[35] M. Moustafa, M.H. Mohd, A.I. Ismail, et al. Dynamical analysis of a fractional order eco-epidemiological model with nonlinear incidence rate and prey refuge, J. Appl. Math. Comput. 65 (2020), 623–650. https://doi.org/10.1007/s12190-020-01408-6.

[36] I. Petras, Fractional-order nonlinear systems: modeling, analysis and simulation, Springer London, Higher Education Press, Beijing, 2011.

[37] H.S. Panigoro, A. Suryanto, W.M. Kusumahwinahyu, et al. Dynamics of a fractional-order predator-prey model with infectious diseases in prey, Commun. Biomath. Sci. 2 (2019), 105-117. https://doi.org/10.5614/cbms.2019.2.2.4.

[38] H.L. Li, L. Zhang, C. Hu, et al. Dynamical analysis of a fractional-order predator-prey model incorporating a prey refuge, J. Appl. Math. Comput. 54 (2016), 435–449. https://doi.org/10.1007/s12190-016-1017-8.

[39] S.K. Choi, B. Kang, N. Koo, Stability for Caputo fractional differential systems, Abstr. Appl. Anal. 2014 (2014), 631419. https://doi.org/10.1155/2014/631419.

[40] A. Boukhouima, K. Hattaf, N. Yousfi, Dynamics of a fractional order hiv infection model with specific functional response and cure rate, Int. J. Differ. Equ. 2017 (2017), 8372140. https://doi.org/10.1155/2017/8372140.

[41] C. Vargas-De-León, Volterra-type Lyapunov functions for fractional-order epidemic systems, Commun. Nonlinear Sci. Numer. Simul. 24 (2015), 75–85. https://doi.org/10.1016/j.cnsns.2014.12.013.

[42] J. Huo, H. Zhao, L. Zhu, The effect of vaccines on backward bifurcation in a fractional order HIV model, Nonlinear Anal.: Real World Appl. 26 (2015), 289–305. https://doi.org/10.1016/j.nonrwa.2015.05.014.

[43] S. Marino, I.B. Hogue, C.J. Ray, et al. A methodology for performing global uncertainty and sensitivity analysis in systems biology, J. Theor. Biol. 254 (2008), 178–196. https://doi.org/10.1016/j.jtbi.2008.04.011.

[44] A. Saltelli, P. Annoni, I. Azzini, et al. Variance based sensitivity analysis of model output. Design and estimator for the total sensitivity index, Computer Phys. Commun. 181 (2010), 259–270. https://doi.org/10.1016/j.cpc.2009.09.018.

[45] K. Diethelm, N.J. Ford, A.D. Freed, A predictor-corrector approach for the numerical solution of fractional differential equations, Nonlinear Dyn. 29 (2002), 3–22. https://doi.org/10.1023/a:1016592219341.